The 2010 IEEE/RSJ International Conference on
Intelligent Robots and Systems
October 18-22, 2010, Taipei, Taiwan

Index finger system force capabilities under simulated pathological conditions

A.B. Sghaier, L. Romdhane, and F.B. Ouezdou, *Member, IEEE*

Abstract— **When dealing with the design of robotic fingers driven by tendons, one can be inspired by the human index finger tendon distribution. The structure of the designed robot finger has to minimize the number of tendons required without sacrificing either the actuated degree of freedom or the maximal output force produced at the fingertip. In this paper, a biomechanical study of the index finger under normal and abnormal conditions is developed. Under abnormal conditions, when some pathology affects the musculo-tendon units, the number of intact muscular actuators will be reduced. A three-dimensional biomechanical model for a static force analysis is developed through anatomical and kinematic studies. An optimization approach is then used to determine muscle force distributions corresponding to maximal fingertip strength when performing isometric force tasks. Further common cases of injured flexors and extensors are analyzed. The simulation method of such abnormalities is described and the results are reported. This investigation allows us to analyze the importance of the tendons distribution in order to enhance the robotic hands design process. In fact, the obtained force distributions are linked to the further required motor torques of the artificial robotic finger driven by tendons. Hence, the developed approach can be with great help whenever the motor sizing process is investigated.**

I. Introduction

The human fingers present a fascinating muscular contrivance. Their ability to coordinate multiple degrees of freedom and to act with simultaneous delicacy and force is the envy of roboticists. In fact, with the aim of designing a tendon-driven robotic hand [1], which can emulate the grasping ability of a human hand, numerous research projects have been conducted [2], [3], [4]. There even have been numerous anthropomorphic robotic hands constructed to allow versatile assembly tasks, to investigate human-like manipulation abilities. The later constitutes an undergoing project carried out by the third author research group at the University of Versailles. This investigation may be also useful in ergonomics where different products and tools need to be adjusted to human grasp in order to minimize hand discomfort and injuries [5], [6]. Clinical treatment and rehabilitation efficiency requires a thorough understanding of the human being finger's motor capabilities [7], as well as its associated functional deficit. The last aspect can increase our understanding of the human's hand complexity since it may be considered as reduced model of a healthy one. Moreover, studying the biomechanical principles of the fingers that govern hand functions in normal and pathological states provides a sound basis for the development of finger joint prostheses [8].

Human finger motor dysfunction resulting from musculoskeletal pathologies, especially tendon disruptions, can severely impair hand function. Thus, the quantification of functional deficit is of paramount importance in evaluating the state of impaired hands. However, studies of the internal force capabilities have often been used when exploring finger dysfunctions. Among the several studies that have been conducted on this subject, the one presented by An *et al.* [9] predicted the forces in the normal and the abnormal hand during isometric hand function, mainly during the pinch function. Valero-Cuevas *et al.* reported the fingertip force reduction in the index finger following paralysis of extrinsic and intrinsic muscles [10]. Toyoda *et al.* simulated the paralysis of intrinsic muscles [11].

The goal of this paper is to extract the crucial features that need to be mimicked to construct a tendon-driven robotic finger minimizing the number of tendons required without sacrificing either the actuated degree of freedom or the force capabilities. As a first step, a static analysis of the healthy and the pathological musculoskeletal system is performed. This leads us to provide an understanding of, on one hand, the system's functionality during loss of tendon and, on the other hand, the muscle functions due to tendon disruptions. The reduction of the ability to produce a strong and well-coordinated pinch due to damaged tendons is also investigated.

A three-dimensional biomechanical model based on robotic principles is detailed in section II. The analytical model describing the relationship the fingertip force and the muscular forces is presented in section III. The optimization procedure and the simulation method of each abnormality are described in section V. The results of the model presenting the effects of the tendon/muscle loss are reported on section VI. The last section gives the conclusion and the further work.

Manuscript received March 10, 2010.

A. B. Sghaier is with the Laboratory of Mechanical Engineering of University of Monastir, TUNISIA, (e-mail: amani.bsghaier@gmail.com).

L. Romdhane is with the Mechanical Engineering of University of Monastir, TUNISIA, (e-mail: lotfi.romdhane@enim.rnu.tn)

F. B. Ouezdou, is with Laboratory of Systems Engineering of Versailles, Université de Versailles, FRANCE, (e-mail: ouezdou@liris.uvsq.fr).

II. INDEX FINGER BIOMECHANICAL MODEL

The forefinger is described as a serial robotic manipulator attached to the palm with four rigid segments (Fig.1) and four DOF [12]. The segments include the index metacarpal bone, the proximal (PP), the middle (MP) and the distal (DP) phalanges. All the joints are assumed to be frictionless. Two hinge joints (one DOF) are used to model the flexion-extension of the proximal interphalangeal (PIP) and the distal interphalangeal (DIP) joints. The two MCP rotational axes are assumed to be fixed with respect to the metacarpal bone, with flexion-extension followed by abduction-adduction. The MCP abduction-adduction axis is not orthogonal with respect to the flexion-extension axis. This axis is assumed to be rotated by 20° in the extension direction in accordance with the literature [12]. The transformation from the MCP to the PIP, and from the DIP to the fingertip, are all defined such that the axes of rotation are parallel.

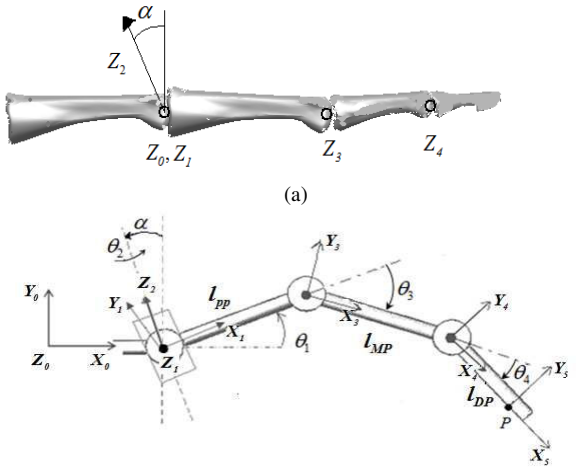

Fig. 1. (a)-(b) Kinematic model of the index finger and depiction of the different coordinate systems and segment lengths. $l_{PP} = 4.9$, $l_{MP} = 3.1$ and $l_{DP} = 2.4$ are the lengths of the proximal, the middle and the distal index finger segments, respectively. θ_4= DIP extension; θ_3 = PIP extension; θ_2=MCP adduction and θ_1 = MCP extension

In Fig. 1b the different coordinate systems and segment lengths used to compute the kinematic model of the index finger are shown. The axes X_0 , Y_0 and Z_0 correspond to the metacarpal bones considered as the global reference frame. The rotational axes (Z_1, Z_2) coincide with the rotational axes of the MCP joint, the flexion-extension and the abduction-adduction axes, respectively. Z_3 and Z_4 represent the flexion/extension axes of the PIP and the DIP joints respectively. X_5 , Y_5 and Z_5 define the axes of the frame fixed to the index fingertip.

The index finger kinematic is driven by seven extrinsic muscles (see Table I), which are responsible for the index finger phalanges movements. For the first phalanx, the flexion movement is actuated by the RI, the UI and the LUM muscles, assisted by the FDP and the FDS muscles.

The extension movement of the first phalanx is controlled by the EDC and the EI muscles, whereas the abduction movement is actuated by the RI muscle and the adduction movement by the UI muscle. The flexion of the second phalanx is actuated by the FDS muscle, and the flexion of the third phalanx is actuated by the FDP muscle.

TABLE I
COMPONENTS INCLUDED IN THE BIOMECHANICAL MODEL

Finger	Muscle	Abbreviation	PCSA (cm²)
Index finger	Flexor digitorium profundus	FDP	4.1
	Flexor digitorium superficialis	FDS	4.2
	Extensor digitorium communis	EDC	1.39
	Extensor indicis	EI	1.12
	Radial interosseous	RI	4.16
	Ulnar interosseous	UI	1.6
	Lumbrical	LUM	0.36

Note: $PCSA_i$ is the physiological cross-sectional area of the i^{th} muscle [9].

The extension of the DIP and PIP joints is actuated by the complex extension apparatus (Fig. 2), which is made of a tendinous extensor network that wraps over the dorsum of the finger's phalanges. The dorsal extensor tendon divides into a central slip (ES) that extends the PIP joint and then into two lateral bands RB and UB that extend the DIP joint.

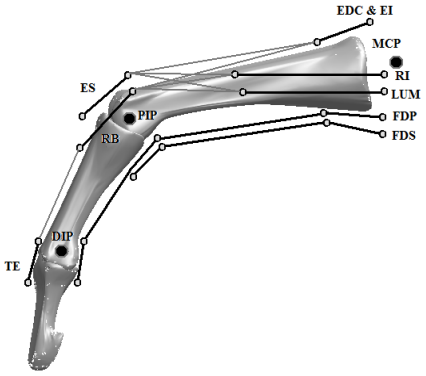

Fig. 2. Schematic representation of tendon junctions of the index finger (radial view).

The force transmitted by the radial band (RB) and the ulnar band (UB) to the terminal extensor (TE) is modeled as (1) [13].

$$F_{TE} = \chi_{RB} F_{RB} + \chi_{UB} F_{UB} \tag{1}$$

The coefficients χ_{RB} and χ_{UB} are the cosine terms, which account for the convergence angles of the RB and UB tendons on the TE one. The numerical values of these coefficients are χ_{RB} = 0.992 and χ_{UB} = 0.995 [13]. The remaining proportions of force transmitted to the extensor mechanism, the unknowns' α_k coefficients (2), vary according to the relative flexion angles of the MCP and the PIP joints [14].

$$\begin{aligned} F_{RB} &= \alpha_{EDC} F_{EDC} + \alpha_{LUM} F_{LUM} \\ F_{UB} &= \alpha_{EDC} F_{EDC} + \alpha_{UI} F_{UI} \\ F_{ES} &= (1-\alpha_{UI}) F_{UI} + (1-\alpha_{LUM}) F_{LUM} + (1-2\alpha_{EDC}) F_{EDC} \end{aligned} \tag{2}$$

F_i defines the tension of the i^{th} muscle.

III. Case Study

We analyze the musculo-skeletal system of the index finger under normal and abnormal conditions. Abnormal conditions are characterized partial and complete by tendon injuries and disruptions. We simulate, particularly, the RI, FDP, FDS, and EDC tendon injuries with different degrees of functional disability. When a tendon is partially disrupted, the remaining intact part can usually sustain forces. Whereas, when a tendon is entirely disrupted, no force passes through it, no matter how hard the corresponding muscle contracts.

IV. Mapping from Muscle Forces to the Fingertip Loading

In the study's simulation, the index finger is placed in closed tip pinch postures (Table II). The axes X_5, Y_5, Z_5, shown in Fig.1 b, are the axes of the reference frame fixed to the index fingertip, and define the distal, the dorsal and the lateral force directions, respectively. The contact between the fingertip and the object is assumed to occur through a single frictionless contact point. Thus, the entire fingertip force is exerted along the normal direction (the dorsal direction in the developed model).

TABLE II
JOINT ORIENTATION ANGLES (DEGREES)

	MCP adduction	MCP extension	PIP extension	DIP extension
Notation	θ_1	θ_2	θ_3	θ_4
Posture 1	0	-45	-45	-10
Posture 2	0	-48	-50	-25

Mathematically, the relationship between the muscle forces and the fingertip loading is represented by the following matrix equation:

$$\mathbf{J}^T \boldsymbol{F}_{ext} = \mathbf{R}\boldsymbol{F} \tag{3}$$

where:

-- $\boldsymbol{F}_{ext}$ is the end-point force vector applied on the fingertip reference frame.

-- $\mathbf{J}^T$ defines the transpose Jacobian 4x6 matrix, which represents the model's skeletal kinematics, transformed fingertip forces into the joint moments [15].

-- **R** moment arm and extensor mechanism interaction matrix which superimposes the joint torque vector produced by each muscle force to obtain the joint torque vector [15].

V. Mathematical Model and Formulation of the Optimization Problem

Based on the above biomechanical model, the index finger is a muscular redundant system. Hence, there is no unique combination of muscular tensions that satisfies the mechanical equilibrium of the finger and balances of the tendon nets. The aim is to determine the distribution of muscle tensions that maximizes the forces exerted on the tip index finger. The resolution is based on an optimization procedure as stated in the following section.

A. Unknown variables

The unknowns variables are the muscle tensions $\boldsymbol{F} = [F_{FDP} \quad F_{FDS} \quad F_{EDC} \quad F_{EI} \quad F_{LUM} \quad F_{RI} \quad F_{UI}]$, in addition to the three unknown coefficients $\boldsymbol{\alpha} = (\alpha_k)$, k=EDC, UI, LUM, which are introduced by equation (2). The tensions of the RB, UB, ES and TE tendons can be computed since the three coefficients (α_k) are determined.

B. Constraints

1) The first constraint represents the limit values of the design variables. The inequality (4) ensures positive muscle tensions, which are lower than the theoretical maximal muscle tensions.

$$0 \le F_i \le F_{\max_i} \le F_{isom_i}, \; i=1,..,7 \tag{4}$$

Where F_{max_i} defines the maximal tension of the i^{th} normal or abnormal muscle. For a normal musculo-tendon unit, the maximal force is equal to the maximal isometric strength, computed as $F_{isom_i} = \sigma PCSA_i$, where the stress σ=35 N/cm² is a constant value reported by Valero-Cuevas et al. [16] for all the musculoskeletal systems of the human upper limb.

$$0 \le \alpha_{UI} \le 1, 0 \le \alpha_{LUM} \le 1, 0 \le \alpha_{EDC} \le 0.5 \tag{5}$$

2) The inequality system (5), as described by Vigouroux et al. [14], states that the factors α_k transmitted by the muscles to the extensor mechanism bands range from 0 to 1 for the LUM and the UI muscles, and from 0 to 0.5 for the EDC muscle.

3) The third constraint considers the fact that the tendon tensions resulting moments must be balanced by the external forces and moments (3).

C. Cost function

We compute the muscles tensions which simultaneously maximize the force exerted on the index fingertip and minimize the quadratic sum of the muscle stress (6) while subjected to the above constraints.

$$f = \sum_{i=1}^{n} (F_i / PCSA_i)^2 \tag{6}$$

D. Resolution method

The developed mathematical model of the index finger in static equilibrium is used to simulate the tendon tension distribution firstly for the healthy finger and secondly for multiple cases of pathological index fingers. These cases will help in identifying the real contribution of the tendons. In our simulation, a search of maximal fingertip capabilities and the corresponding tendon tension distributions is performed. Using the optimization method, the unknown vector [**F**, **α**] that minimize the muscle stress sum (8) and maximize the output fingertip force for a given joint

configuration are computed. To calculate the maximal external finger force which can be applied in a specific pinch posture, the associated magnitude is also treated as an additional unknown variable in the optimization process.

The same model is then modified to define various abnormal states of the index finger. In our analytical model, these investigated abnormal conditions are based mathematically on the reduction of the corresponding muscle strength. Systematic reduction of muscle strengths is introduced by assigning appropriate values to the upper bounds of the involved muscle forces. Then the corresponding maximal functional output fingertip force is calculated for each amount of reduction. For each simulated abnormality, when the muscle/tendon is completely disrupted, the associated force is neutralized.

VI. Simulation Results

A. Maximum fingertip force for each pathology

Under normal conditions, where all the tendons are intact, the simulated values of the pinch strength for the studied postures (1 and 2) are 58N and 36N, respectively. The magnitude of the simulated fingertip forces falls within the range of maximal tip forces (19-106N), which is reported by An *et al.* [9].

The simulation of the RI muscle loss shows that output force capability of close to normal could be produced for a reduction of less than 40% of the RI strength loss (Fig. 3) for the two postures. If the RI strength loss is greater than 40%, maximal output strength decreases significantly in posture 1.

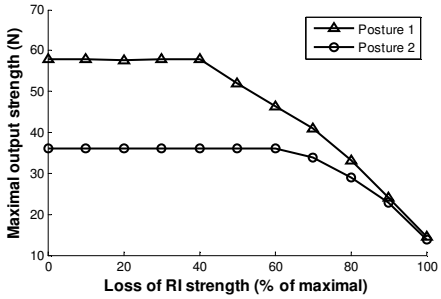

Fig. 3. Reduction of maximal output force due to the loss of the RI muscle/tendon strength (Posture 1, Posture 2).

Although, individually the intrinsic muscles as RI, LUM are small muscles in diameter, collectively they represent a large contribution in output force strength. In fact, when the RI tendon is completely disrupted, the index finger generates a weak output pinch force strength, 14N (Fig. 3), i.e. 24% of the value of its normal maximal strength. This result is close to the one estimated by An *et al.* [9]. An *et al.* reported that a complete loss of the RI force capability yields a maximal tip pinch strength which is equal to 25% of the normal strength.

The simulation of the FDP muscle loss shows that the dysfunction of the FDP musculo-tendon unit consequently leads to impaired fingertip strength. For the two studied postures, the pinch task is unfeasible following a complete disruption of the FDP tendon. When the FDP muscle becomes completely inactive, no pinch force can be generated (Fig. 4), since the DIP joint has lost its active flexion and it is no longer able to maintain its normal joint configuration.

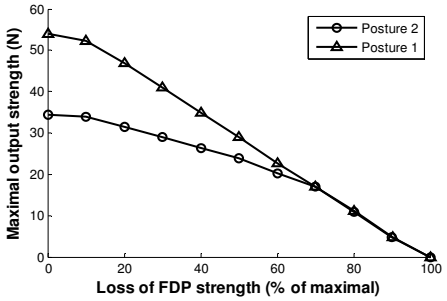

Fig. 4. Reduction of maximal output force due to the loss of the FDP muscle/tendon strength.

In the case of the FDP strength loss, the evaluated output force capability is lower than the one associated to the RI strength deficit. In Fig. 4, the maximal strength of the output pinch force shows a linear decrease versus the loss of FDP strength. For a deficit of FDP force capability equal to 50%, the output strength reduction for posture 1 and 2 are 50% and 33%, respectively, in comparison with a normal index finger. For high-grade injuries, when the FDP strength reduction is at least 70% of the normal index finger, the maximal output force is significantly reduced. It is equal to zero for a complete FDP tendon disruption. Partially injured tendons should not be repaired if at least 30-40% of the tendon remains intact. The intact part of the tendon can usually sustain output forces with different grades.

For FDS high-grade injuries and even for a complete disruption of the FDS musculo-tendon unit, the production of a functional endpoint force is still possible due to compensation ability of other muscles higher tensions (Fig.5). The FDS rupture induces weakened maximal output strength which is equal to 14N for the studied postures.

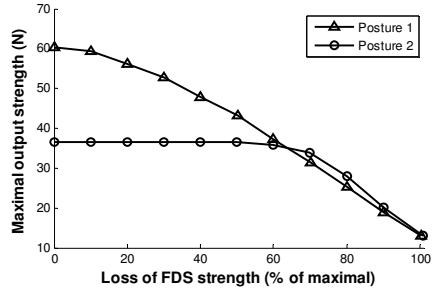

Fig. 5. Reduction of maximal output force due to the loss of the FDS muscle/tendon strength.

Disruptions involving less than 30% of EDC muscle strength loss cannot influence the output strength capability (Fig. 6). This is due to the compensatory contractile force of the EI muscle remaining intact. The extensor EI is progressively activated as the loss of the EDC strength is more important. On the other hand, high-grade injuries of the EDC tendon reduce significantly the magnitude of

maximal fingertip force. The complete disruption of the EDC tendon produces a deficit of the output strength that is equal to 40% in comparison with a normal index finger case. When both extensors, EDC and EI, are completely disrupted, the deficit is even more important, and it is equal to almost 97%. A partial disruption of EDC and EI extensors leading to a 70% loss of EDC and EI strengths reduces maximal output force by 15% (Fig. 6).

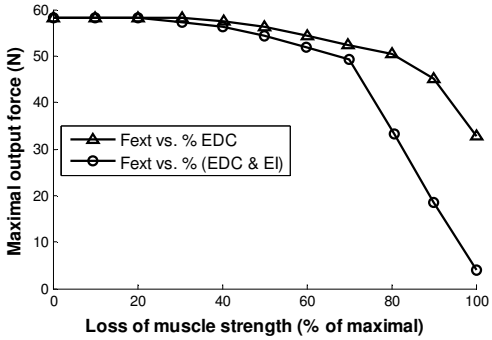

Fig. 6. Reduction of maximal output force due to the loss of the EDC, EDC& EI muscle/tendon strength (Posture 1).

B. Tendon forces distribution for each pathology

Under normal conditions, forces as high as four times the applied external force are assumed to be present along the flexor tendons. This value is lower than 7.92 (6.33) as measured by Schuind *et al.* [17] and higher than the predicted values (1.93-2.08) as reported by the same authors. These variations are probably due to the fact that the studied postures are not necessarily similar to Shuind one.

When evaluating the impact of RI strength deficit, muscle tension distribution remains invariable up to 40% of the RI strength loss (Fig. 7). The loss of the RI tendon reduces the ability to maintain the radial-ulnar balance of the MCP joint. For each partial RI tendon disruption, the compensatory mechanism among the remaining muscles maintains a possible functional output force and a new state of balance is established. Each state favors a new distribution of tensions among the intact muscles. The substantial increases in normalized muscle forces indicate that the estimated output force would be significantly reduced. Beyond 40% of RI strength loss, the FDP, EDC, LUM tendons get progressive ratios.

In particular, the partial disruption of RI increases the LUM strength, which is initially inactive when the RI is intact. In fact, the LUM as an MCP abductor has an effect similar to the one of RI. The strength of the LUM, combined with the one of the EDC, compensates the lost of RI and ensures the MCP joint balance.

The contribution of the RB and UB bands increases, therefore the force transmitted to the TE tendon also grows. The UI and EI muscles are not actively involved in the production of output force. The normalized tensions of FDS and ES decrease continually (Fig. 7). From 70% of RI strength loss, the ES muscle is completely inactive.

Rupture of a finger flexor tendon can be a significant injury, leading to marked functional impairments. In the case of a complete FDP loss, for instance, the remaining healthy muscles fail to compensate the FDP action.

Following the complete FDP disruption, no changes are noted for other tendon tension ratios (Fig. 8).

The functional loss, resulting from the FDS rupture or the FDS partial disruption, is minimal compared to that of FDP rupture.

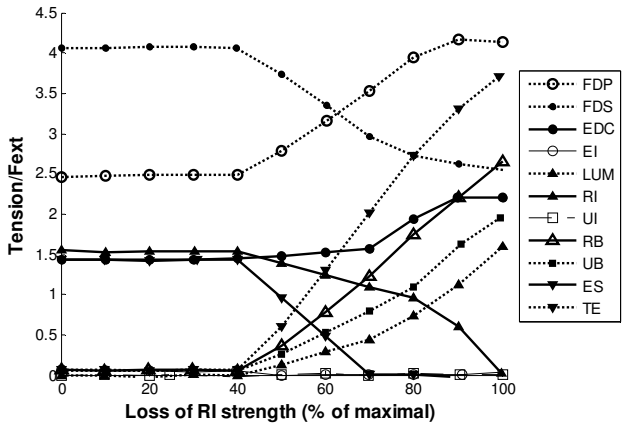

Fig. 7. Muscle forces (in units of applied force) of index finger under external loading corresponding to the reduction in the RI force capability (Posture 1).

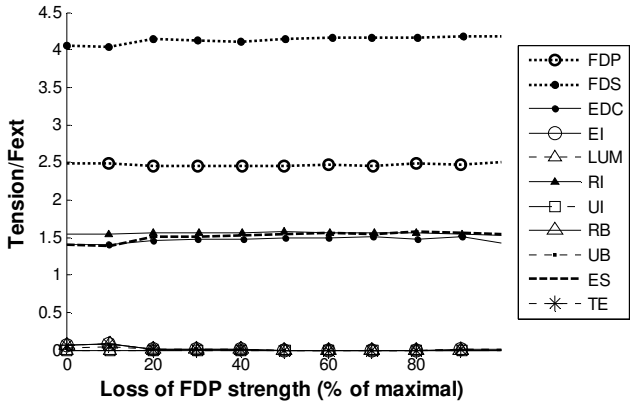

Fig. 8. Muscle forces (in units of applied force) of the index finger under external loading corresponding to the reduction in the FDP force capability (Posture 1).

For different grade of the FDS disruption, all the musculo-tendon units, excepting the ES tendon, provide increased normalized tensions. The contribution of the ES is completely zero from 50% of FDS strength reduction (Fig. 9). The intrinsic muscles, in particular, appear to produce large force during pinch grasp, to stabilize the MCP joint.

When the EDC tendon is partially disrupted, the index finger preserves the same tension distribution till 30% of EDC strength loss (Fig. 10). This constancy is due to the presence of the other extrinsic extensor, mainly. In fact, the EI muscle fills the same functionality as the EDC muscle.

However, for EDC strength loss that is higher than 30%, the tendon distribution changes as much as the grade of loss increases, even with EI tendon tension increase. Moreover, normalized tensions of the RB, UB, and TE increase. Since the ES tendon is piloted by EDC and EI muscles, its

associated tension is also reduced. To guarantee the balance of MCP joint, the FDS normalized tension diminishes as much as the counteraction of the long extensor is lost.

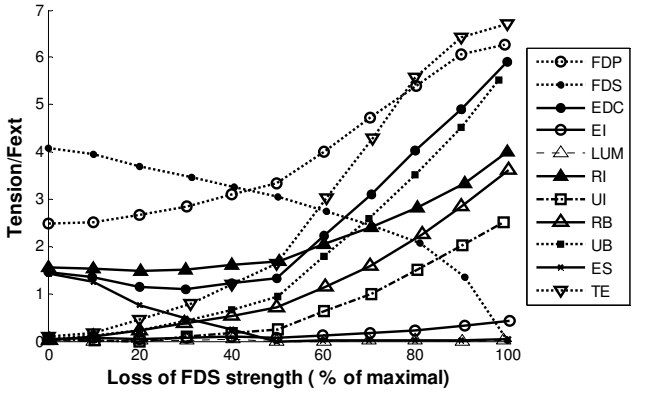

Fig. 9. Muscle forces (in units of applied force) of index finger under external loading corresponding to the reduction in the FDS force capability (Posture 1).

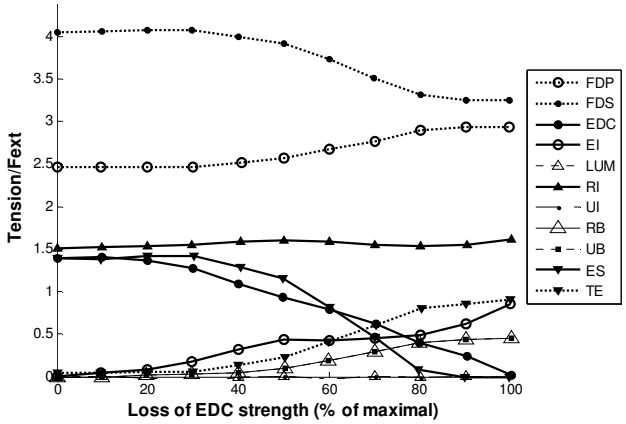

Fig. 10. Muscle forces (in units of applied force) of index finger under external loading corresponding to the reduction in the EDC force capability (Posture 1).

VII. Conclusions

The simulation of different abnormal muscle or tendon conditions aims to explore the feasibility of using a mathematical model to study the pathologies of the index finger and the resulting functional forces. These results permit a better understanding of the utility of each muscle/tendon, including those of the extension mechanism.

We identified many crucial features of the musculo-skeletal system that need to be mimicked to construct an anatomical robotic finger. Studying pathological fingers allow us to assess the impact of muscles strengths reductions on the amount of the resulting fingertip force. Consequently, we can conclude the minimal number of cable-driven actuators, which are necessary to control the different finger joints and to ensure a desired fingertip force.

The investigation of the underlying pathological mechanisms of human finger may also have significant implications for the choice of adequate reconstructive surgical procedures such as tendon transfers. The above-mentioned issues constitute the further developments of the proposed study and are currently investigated in our research group.

References

[1] S.Y. Jung, S.K. Kang, M.J. Lee and I. Moon, "Design of Robotic Hand with Tendon-driven Three Fingers," in *Proc. the IEEE international conference on Control, Automation and Systems,* ICCAS '07, pp 83–86, Korea, 2007.

[2] T. Hino and T. Maeno, "Development of A Miniature Robot Finger with A Variable Stiffness Mechanism Using Shape Memory Alloy," Nippon Robotto Gakkai Gakujutsu Koenkai Yokoshu, vol. 22, pp. 3-24, 2004.

[3] Y.W. Liu, H.G. Wang, B. Li and W. Zhou The underactuation and motion-coupling in robotic fingers and two new 1-DOF motion-coupling anthropomorphic fingers. In: *Proc. the IEEE International Conference on Robotics and Biomimetics*, vol. 1-4 pp.1573–1578, Thailand, 2009.

[4] G. Stellin *et al.*, "Preliminary Design of an Anthropomorphic Dexterous Hand for a 2-Years-Old Humanoid: towards Cognition," in *Proc. the IEEE International Conference on Biomedical Robotics and Biomechatronics, BioRob*, pp. 290-295, Italy, 2006.

[5] N.A. Incel, E. Ceceli, P.B. Durukan, H.R. Erdem, and Z.R. Yorgancioglu, "Grip strength: effect of hand dominance," *Singapore Med J*, vol. 43 (5), pp. 234-237, 2002.

[6] C.S. Edgren, R.G. Radwin, and C.B. Irwin, "Grip force vectors for varying handle diameters and hand sizes," *Hum. Factors*, vol. 46 (2), pp. 244-51, 2004.

[7] J. Chalfoun, R. Younes, M. Renault, and F. B. Ouezdou, "Forces, activation and displacement prediction during free movement in the hand and the forearm," *J. Robotic Systems*, vol. 22 (11), pp. 653-660, 2005.

[8] T.H. Pylios and D.E.T Shepherd, "A New Metacarpophalangeal Joint Prosthesis," *In Proc. of the World Congress on Engineering* , vol. II, pp. 1443-1445 WCE 2007, U.K, 2007.

[9] K. N. An, E. Y. Chao, W. P. Cooney, and R.L. Lincheid, "Forces in the normal and abnormal hand," *J. Orthopaedic Research*, vol. 3, pp. 202-211, 1985.

[10] F. J. Valero-Cuevas, J. D. Towles, and V. R. Hentz, "Quantification of fingertip force reduction in the forefinger following simulated paralysis of extensor and intrinsic muscles," *J Biomech.*, vol. 33 (12), pp.1601-1609, 2000.

[11] H. Toyoda, N. Yamazaki, "Evaluation of finger tendon transfer surgery using the two dimensional link model simulating paralysis of Intrinsic muscle," *Trans. of the Japan Society of Mechanical Engineers*, vol.72 (722), pp. 3272-3279, 2006.

[12] D. G. Kamper, H. C. Fischer and E.G. Cruz, "Impact of finger posture on mapping from muscle activation to joint torque," *Clinic. Biomech*., vol. 21, pp. 361-369, 2006.

[13] An KN, Chao EY, Cooney WP and Linscheid RN, "Normative model of human hand for biomechanical analysis," *J Biomech*, vol. 12 (10), pp.775–788, 1979.

[14] L. Vigouroux, F. Quaine, A. Labarre-Vila and F. Moutet, "Estimation of finger muscle tendon tensions and pulley forces during specific sport-climbing grip techniques," *J Biomech*, vol. 39 (14), pp. 2583-2592, 2006.

[15] A.B. Sghaier, L. Romdhane and F.B. Ouezdou, "A biomechanical analysis of the healthy and the pathological index finger during pinch function," *IEEE/RSJ International Conference Intelligent on Robots and Systems*, *IROS 2008*, pp. 1784-1789, France, 2008.

[16] F.J. Valero-Cuevas, M.E. Johanson and J.D. Towles, "Towards a realistic biomechanical model of the thumb: the choice of kinematic description may be more critical than the solution method or the variability/uncertainty of musculoskeletal parameters," *J Biomech*, vol. 36 (7), pp.1019–1030, 2003.

[17] F. Schuind, M. Garcia-Elias, W.P. Cooney, K.N. An, "Flexor tendon forces: in vivo measurements," *J Hand Surg.*, vol. 17, pp.291-298, 1992.